Diagnostic Accuracy of Scanning Laser Polarimetry with Enhanced versus Variable Corneal Compensation

T. A. Mai, MD, N. J. Reus, MD, PhD, H. G. Lemij, MD, PhD

Purpose: To compare the diagnostic accuracy of scanning laser polarimetry (SLP) parameters between images taken with enhanced corneal compensation (ECC) and those with variable corneal compensation (VCC) and to explore the effect of atypical birefringence patterns on this accuracy.

Design: Cross-sectional observational study.

Participants: Forty-one healthy subjects and 92 patients with primary open-angle glaucoma.

Methods: Variable corneal compensation and ECC images were obtained of 1 eye per subject, selected randomly if both eyes were eligible. For both ECC and VCC, the areas under the receiver operating characteristic curves (AUROCs) and the sensitivity at a specificity of ≥95% were calculated per parameter in all eyes. The analyses were reperformed separately in eyes with and without atypical birefringence patterns (ABP) images.

Main Outcome Measures: The AUROCs and sensitivities at a specificity of ≥95% for various SLP parameters in all eyes and in eyes without ABP images.

Results: The diagnostic accuracy for most standard parameters (temporal-superior-nasal-inferior-temporal [TSNIT] average, superior average, inferior average, and TSNIT standard deviation) in all eyes was statistically significantly higher with ECC than with VCC, except for the nerve fiber indicator (NFI). When only eyes without ABP were used for the analysis, the diagnostic accuracy of SLP parameters with VCC improved, and the differences in diagnostic accuracy between ECC and VCC for these parameters lost their statistical significance.

Conclusions: Standard SLP parameters (except for the NFI) generally had a higher diagnostic accuracy when eyes were imaged with ECC than with VCC because there were fewer ABP images with ECC than with VCC. Enhanced corneal compensation therefore may be more reliable than VCC for the detection of glaucoma. A future automated classifier, similar to the current NFI, may perform better if it is trained on data obtained with ECC. Clinically, retinal nerve fiber layer images with marked ABP, acquired with either ECC or VCC, should be viewed with caution. *Ophthalmology 2007;114:1988–1993 © 2007 by the American Academy of Ophthalmology.*

In recent years, scanning laser polarimetry (SLP) has emerged as a promising imaging technique to quantitatively assess retinal nerve fiber layer (RNFL) thinning caused by, for instance, primary open-angle glaucoma, a progressive optic neuropathy caused by degeneration of retinal ganglion cells and their axons.[1–4] Scanning laser polarimetry is a noninvasive, noncontact imaging technology that allows indirect quantification of the RNFL thickness through RNFL retardation, a measurable phase shift of polarized light passing through the presumed form birefringent RNFL that is known to relate linearly to measured RNFL thickness.[5] Because the anterior segment, mostly the cornea, also exhibits form birefringence, SLP with variable corneal compensation (VCC; commercially available as GDx VCC [Carl Zeiss Meditec, Inc., Dublin, CA] has been introduced to neutralize the confounding effects of eye-specific corneal birefringence on RNFL retardation measurements.[6–8] With the GDx VCC, RNFL retardation has been shown to correlate well with visual field sensitivity,[9–11] as well as with other imaging techniques.[12–16] Also, the power to discriminate between healthy and glaucomatous eyes is better with VCC than with its predecessor, SLP with fixed corneal compensation.[17–19] However, atypical birefringence patterns (ABPs), as seen in a subset of normal and glaucomatous eyes, may confound the RNFL thickness measurement by VCC.[20] Variable corneal compensation images with ABPs are characterized by an atypical retardation map, with variable areas of high retardation arranged in a spokelike peripapillary pattern, or splotchy areas of high retardation nasally and temporally.[20] Quantitatively, any presence of ABPs is indicated by a support vector machine (SVM)-derived[20] typical scan score of less than 80 (total range, 0–100).[21,22] Atypical birefringence patterns may be related to age, myopia, and blond fundi. A suggested cause

Originally received: September 6, 2006.
Final revision: January 24, 2007.
Accepted: January 25, 2007.
Available online: April 24, 2007. Manuscript no. 2006-1010.

From Rotterdam Eye Hospital, Rotterdam, The Netherlands.

Supported by Rotterdam Eye Hospital Research Foundation, Rotterdam, The Netherlands.

Drs Mai, Reus, and Lemij received research support at no cost from Carl Zeiss Meditec, Dublin, California, through Rotterdam Eye Hospital. Dr Lemij also serves as a consultant for Carl Zeiss Meditec.

Correspondence to T. A. Mai, MD, Rotterdam Eye Hospital, Schiedamse Vest 180, 3011 BH Rotterdam, The Netherlands. E-mail: tamai@eyehospital.nl.

ISSN 0161-6420/07/$–see front matter
doi:10.1016/j.ophtha.2007.01.022

of ABP is a low signal-to-noise ratio resulting from lost or attenuated reflectivity of the retinal pigment epithelium.[20]

Scanning laser polarimetry with enhanced corneal compensation (ECC), the latest software change of the GDx, has been introduced to optimize SLP imaging by improving the signal-to-noise ratio, notably in areas with a low signal. It was first described by Knighton and Zhou,[23] who assumed that the susceptibility of SLP to error, both optical (e.g., stray light) and electronic (e.g., noise, digitization error), is relatively large when the sensitivity of SLP to small retardation differences is low (low retardance, depolarization, or reduction in reflected intensity). The sensitivity of SLP to the main signal is increased by adding a predetermined birefringence (bias retarder) during image acquisition, allowing the total retardation to be shifted into a more sensitive region of the device's detector to the polarization signal amplitude. The RNFL retardation then is calculated by subtracting corneal plus bias retardance from the total retardance. With ECC, ABPs seem to be less frequent and less severe compared with VCC.[21–23] However, little is known about whether the diagnostic accuracy also would improve with ECC compared with VCC.

The purpose of the current study was to compare the diagnostic accuracy of the SLP parameters between ECC and VCC and to examine any effect of ABPs on this diagnostic accuracy. Because ECC was introduced to improve the signal-to-noise ratio of SLP imaging, the diagnostic accuracy with ECC was expected to be better than with VCC.

Patients and Methods

Participants

One hundred thirty-three participants, consisting of 41 healthy subjects and 92 glaucoma patients, all of white ethnicity, took part in this study. Of these individuals, 60 (45.1%) were women. Seventy (52.6%) of the selected eyes were right ones. Healthy individuals and glaucoma patients had a mean age±standard deviation of 61.2±12.0 years and 65.4±10.9 years, respectively. Neither the difference in age (4.1±2.1 years), gender (5.3%), nor eye side (5.6%) between the healthy and glaucoma groups was statistically significant ($P = 0.54$, 2-tailed independent samples Student t tests; $P = 0.55$ and $P = 0.57$, chi-square test). All subjects underwent a complete ophthalmologic examination, including slit-lamp biomicroscopy, intraocular pressure measurement by Goldmann applanation tonometry, gonioscopy, and a white-on-white standard automated perimetry visual field (VF) test (commercially available Humphrey Field Analyzer; Carl Zeiss Meditec, Inc.). The used VF testing strategy was either 24-2 full-threshold (in 126 subjects), 24-2 standard Swedish Interactive Testing Algorithm (in 5 subjects), or 24-2 fast Swedish Interactive Testing Algorithm (in 2 subjects). None of the subjects had a history of ocular disease (except glaucoma in the glaucoma group), intraocular surgery (except uncomplicated cataract surgery), or significant coexisting systemic diseases with possible ocular involvement, such as diabetes mellitus or arterial hypertension. Only 1 eye per subject was selected randomly if both were eligible. All selected eyes had a best-corrected visual acuity of 20/40 or better. The range of spherical equivalent refractive error in the subject population was between –7.0 diopters (D) and 3.0 D. For healthy individuals, only VFs that met reliability criteria of fixation losses less than 25% and false-negative and false-positive responses of 20% or less were included. For the glaucoma subjects, the same criteria for inclusion of the VFs were applied, except that a margin of up to 33% false-negative responses were considered to be acceptable. All protocols and methods used in the present study adhered to the tenets of the Declaration of Helsinki and were approved by the Institutional Human Experimentation Committee. Informed consent was obtained after the participants were informed about possible consequences of the study.

Healthy subjects were recruited consecutively either from an ongoing longitudinal follow-up study of the Rotterdam Eye Hospital or from staff members, their friends and spouses, partners of the patients, or volunteers. All healthy subjects had unremarkable slit-lamp examination results, open angles on gonioscopy, an intraocular pressure of 21 mmHg or less in both eyes, normal VF test results by standard automated perimetry, a healthy-appearing optic disc (no diffuse or local rim thinning, cupping, or optic disc hemorrhages), and no other ocular abnormalities. Normal VF test results were defined as a mean deviation and a pattern standard deviation within 95% confidence limits and glaucoma hemifield test results within normal limits. None of our healthy subjects reported having first- or second-degree family members with glaucoma. The mean±standard deviation of mean deviation and pattern standard deviation were 0.4±1.1 dB and 1.7±0.4 dB, respectively.

The glaucoma patients had, in their selected eye, a glaucomatous appearance of the optic disc (diffuse or local rim thinning or cupping, possibly with optic disc hemorrhages), a nerve fiber bundle standard automated perimetry VF defect confirmed on 2 consecutive occasions, open angles by gonioscopy, and no evidence of secondary glaucoma. A VF defect in the present study was considered as glaucomatous if it had 2 or more adjacent points at a $P<0.01$ level or deeper, or 3 or more adjacent points at a $P<0.05$ level or deeper in the total deviation plot, or glaucoma hemifield test results outside normal limits not attributable to causes other than glaucoma. Their mean±standard deviation of mean deviation and pattern standard deviation were –9.4±7.4 dB and 8.1±3.9 dB, respectively. The glaucoma eyes were classified by the severity of VF defects described by Hoddapp et al.[25] Of the glaucomatous eyes, 59 (64.1%) were considered to have mild and moderate and 33 (35.9%) were considered to have severe VF defects.

Image Acquisition

All subjects were imaged with SLP with both VCC and ECC (GDx VCC software version 5.4.0 and GDx ECC software version 5.5.0.11; Carl Zeiss Meditec, Inc.). Details of the SLP device have been described elsewhere.[26] In short, the GDx VCC is a modified SLP system using a near infrared laser (785-nm wavelength) to scan the ocular fundus. It is equipped with 2 adjustable linear retarders in rotating mounts that allow eye-specific compensation of corneal polarization axis and corneal polarization magnitude (i.e., retardance) based on the macular retardance profile.[6,27] The RNFL retardation (in nanometers) is calculated taking the retarder-adjusted eye-specific corneal polarization axis and corneal polarization magnitude into account, and then is converted into thickness values (in micrometers) based on a fixed conversion factor of 0.67 nm/μm.[27]

In the ECC mode, a large known bias retarder is introduced so that the combination of corneal plus bias retardance becomes close to 55 nm and with a slow axis close to vertical, allowing the retardation measurement to be shifted into a region where the SLP detector is more sensitive to the backscattered light. The RNFL retardation then is determined by mathematically

subtracting the macular and bias retarder-induced birefringence from the total retardance.[23,24]

In the present study, GDx measurements of both eyes of all subjects were performed by 2 trained and experienced technicians following a standard protocol. Images were scanned through undilated pupils while the room was lit. The subjects were asked to keep their head still during the entire session, with their faces resting on the face mask to allow the best alignment between the instrument's anterior segment compensator and the position of their eyes. The spherical equivalent refractive error of each eye was entered into the instrument, and adjustments in 0.25-D steps were made manually, if required, to allow a proper focus on the retina. The anterior segment birefringence then was determined. Next, images of the RNFL were obtained, first with VCC and then with ECC. A fixed-size band 8 pixels wide (equivalent to 0.4 mm in an emmetropic eye), with inner and outer diameters of 2.4 mm and 3.2 mm, respectively, was centered on the optic nerve head. Retardation values then were calculated within the band to yield 256 values. These values subsequently were grouped into 64 peripapillary points by the software, allowing 5 standard parameters to be calculated, namely, temporal-superior-nasal-inferior-temporal average, superior average, inferior average, temporal-superior-nasal-inferior-temporal standard deviation, and the nerve fiber indicator (NFI). The NFI is an SVM classifier representing the possibility of having glaucoma in an eye based on a large sample of normal and glaucomatous eyes.[28] Only images of high quality (i.e., those with a centered optic disc, well focused, evenly and justly illuminated throughout the image, without any motion artifacts, and with an inbuilt quality scan score of 7 or more) were selected.

Statistical Analysis

The diagnostic accuracy of each SLP parameter was compared between images obtained with ECC and those obtained with VCC. For 5 standard parameters, we constructed receiver operating characteristic curves. The areas under the receiver operating characteristic curve (AUROCs) then were calculated per parameter. Each AUROC represented the ability of an SLP parameter to differentiate glaucomatous from healthy eyes. A value of 1.0 shows perfect discrimination, whereas an AUROC of 0.5 represents chance discrimination. The statistical difference in AUROCs for each parameter between ECC and VCC was tested with the paired test described by DeLong et al.[29]

We also calculated sensitivities at a specificity of 95% or more for each GDx ECC and GDx VCC parameter. The 95% confidence interval of the sensitivity per parameter was approximated with the formula:

$$p \pm 1.96 * \sqrt{p\,(1-p)/n},$$

where p represents the sensitivity and n represents the sample size. For this approximation to be valid, $n * p$ should not be less than 5.[30] The statistical significance of any difference in sensitivities for each parameter between ECC and VCC was tested with the McNemar test for paired proportions.

We also performed the same analyses in eyes without ABPs. An ABP image was defined as one having a typical scan score of less than 80.[21,22] In the current study, a P value of 0.05 was considered statistically significant. All statistical analyses were performed using SPSS software (version 14.0.2 for Windows; SPSS, Inc., Chicago, IL) and Microsoft Excel (Microsoft Excel 2000, SR-1; Microsoft, Redmond, WA).

Results

In all eyes taken together, the diagnostic accuracy of most parameters was statistically significantly higher when the images were obtained with ECC than when obtained with VCC (Table 1). However, for the NFI, the best performing parameter in both ECC and VCC, no such difference between ECC and VCC was found.

The ABP images more often were present in images obtained with VCC than those obtained with ECC (Table 2). When only eyes without ABP were used for the analysis, the diagnostic accuracy of most parameters improved with VCC to a statistically similar level as with ECC (Tables 1, 3). However with both ECC and VCC, the diagnostic accuracy of the NFI was little affected by removing the ABP images (Fig 1).

Table 1. Diagnostic Accuracy of Various GDx Parameters in All Eyes (n = 133 [92 Glaucomatous])

GDx Parameter	Enhanced Corneal Compensation Area under the Receiver Operating Characteristic Curve (Standard Deviation, Range)	Variable Corneal Compensation Area under the Receiver Operating Characteristic Curve (Standard Deviation, Range)	Difference in Area under the Receiver Operating Characteristic Curve	*P* Value*	Enhanced Corneal Compensation Sensitivity % (95% Confidence Interval) at Specificity = 95%	Variable Corneal Compensation Sensitivity % (95% Confidence Interval) at Specificity = 95%	*P* Value†
Nerve fiber indicator	0.986 (0.007, 0.97–1.0)	0.993 (0.004, 0.98–1.0)	−0.01	0.3747	95 (91–98)	98 (95–100)	0.774
TSNIT average	0.98 (0.01, 0.96–1.0)	0.89 (0.03, 0.83–0.94)	0.09	<0.001	90 (85–95)	74 (66–81)	0.001
Superior average	0.98 (0.01, 0.97–1.0)	0.95 (0.02, 0.92–0.98)	0.03	0.0165	87 (81–93)	87 (81–93)	1.00
Inferior average	0.93 (0.02, 0.89–0.97)	0.83 (0.04, 0.76–0.90)	0.10	<0.001	65 (57–73)	52 (44–61)	0.011
TSNIT standard deviation	0.97 (0.01, 0.95–1.0)	0.92 (0.02, 0.87–0.97)	0.05	0.0051	77 (70–84)	58 (49–66)	0.001

TSNIT = temporal-superior-nasal-inferior-temporal.
*Statistical difference in areas under the receiver operating characteristic curve per parameter between enhanced corneal compensation and variable corneal compensation, tested with the paired test after DeLong et al.[29]
†Statistical difference in sensitivities at a set specificity of ≥95% between enhanced corneal compensation and variable corneal compensation, tested with the McNemar test.

Table 2. Distribution of Images with Atypical Birefringence Patterns in Scanning Laser Polarimetry Images with Enhanced and Variable Corneal Compensation in the Study Groups

	Enhanced Corneal Compensation			Variable Corneal Compensation		
	Glaucoma	*Normal*	*All Combined*	*Glaucoma*	*Normal*	*All Combined*
Eyes with ABP images (%)	3/92 (3.3)	0/41 (0)	3/133 (2.3)	39/92 (42.4)	10/41 (24.4)	49/133 (36.8)

ABP = atypical birefringence pattern.

Discussion

In this study, we demonstrated that ECC generally improved the diagnostic accuracy of SLP parameters, compared with VCC. This improvement was the result of fewer ABP images having been obtained with ECC than with VCC. By contrast, the diagnostic accuracy of the NFI was similar for ECC and VCC.

Scanning laser polarimetry has evolved in recent years. Its successive generations have all been capable of differentiating between healthy and glaucomatous eyes.[17–19,31–33] However, ABPs may occur in SLP images. Images without ABPs appear to reflect better the true RNFL morphologic features than those with ABPs.[21–23] Not surprisingly, we found that ABPs also reduced the diagnostic accuracy of most SLP parameters. Therefore, the clinical usefulness of the GDx VCC is enhanced when images with marked ABPs (typical scan score, <80) are disregarded. Alternatively, glaucoma management may benefit from the introduction of ECC, because ABPs occur less often and less markedly with ECC than with VCC. In addition, it is unclear to what extent the presence of ABP may have affected any differences in previously reported diagnostic accuracy of SLP parameters across studies. In future studies, reporting the amount of marked ABP will facilitate the comparison of results between studies.

It is unclear whether eyes with ABPs exist in the GDx VCC normative database, and if so, to what extent. If they indeed have been included in the normative data, they may have to be removed to optimize the classifying ability of most SLP parameters.

The diagnostic accuracy of the NFI perhaps was surprisingly similar for ECC and VCC images, regardless of any ABPs in the images. A possible explanation for this finding may be that areas of VCC images that carry a large weight in the NFI's underlying SVM are those that are little affected by atypical birefringence. However, the robustness of the current NFI for images with marked ABPs does not necessarily mean that it should be used as an important classifier for ECC images because its SVM was trained on VCC data. Whether a future classifier, based on ECC images only, will outperform the current NFI remains to be seen. Because the other parameters served as better classifiers with ECC than with VCC, the authors are in favor of acquiring normative ECC data and developing new classifiers. As with the NFI, it is possible that they then will discriminate better between healthy and glaucomatous eyes than currently with the VCC database.

Although SLP parameters with both ECC and VCC in the current study had a relatively high diagnostic accuracy, it is possible that they will not perform as well in unselected eyes with, for example, myopic optic nerve heads, a myelinated RNFL, scleral crescents, and so forth. Such more

Table 3. Diagnostic Accuracy of Various GDx Parameters in Eyes without Atypical Birefringence Patterns Images (n = 84 Eyes [53 Glaucomatous])

GDx Parameter	Enhanced Corneal Compensation Area under the Receiver Operating Characteristic Curve (Standard Deviation, Range)	Variable Corneal Compensation Area under the Receiver Operating Characteristic Curve (Standard Deviation, Range)	Difference in Area under the Receiver Operating Characteristic Curve	*P* Value*	Enhanced Corneal Compensation Sensitivity % (95% Confidence Interval) at Specificity = 95%	Variable Corneal Compensation Sensitivity % (95% Confidence Interval) at Specificity = 95%	*P* Value†
Nerve fiber indicator	0.987 (0.009, 0.97–1.0)	0.998 (0.002, 0.99–1.0)	−0.01	0.1206	94 (89–99)	98 (95–100)	0.688
TSNIT average	0.98 (0.01, 0.95–1.00)	0.99 (0.01, 0.97–1.00)	−0.01	0.5594	93 (87–98)	87 (80–94)	0.453
Superior average	0.99 (0.01, 0.97–1.00)	0.99 (0.01, 0.97–1.00)	−0.001	0.9309	87 (80–94)	94 (89–99)	0.219
Inferior average	0.95 (0.02, 0.90–0.99)	0.93 (0.03, 0.88–0.98)	0.01	0.3606	76 (66–85)	76 (66–85)	1.00
TSNIT standard deviation	0.97 (0.02, 0.95–1.0)	0.94 (0.02, 0.89–0.99)	0.04	0.0713	66 (56–76)	66 (56–76)	1.0

TSNIT = temporal-superior-nasal-inferior-temporal.
*Statistical difference in areas under the receiver operating characteristic curve per parameter between enhanced corneal compensation and variable corneal compensation, tested with the paired test after DeLong et al.[29]
†Statistical difference in sensitivities at a set specificity of ≥95% between enhanced corneal compensation and variable corneal compensation, tested with the McNemar test.

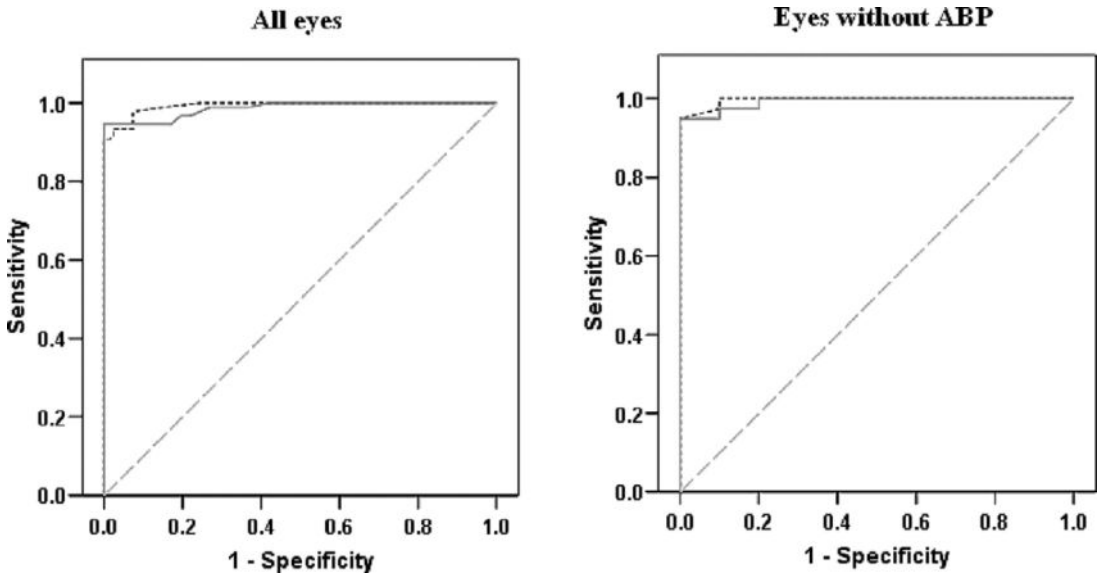

Figure 1. Receiver operating characteristic curves for the nerve fiber indicator with enhanced (solid line) and variable (dotted line) compensation in all eyes and in eyes without atypical birefringence pattern (ABP) images. Dashed line, reference.

realistic conditions may pose a challenge to clinicians managing glaucoma. Exploring the diagnostic accuracy of SLP in unselected eyes may be addressed in future studies.

In conclusion, images with ABP were seen less frequently with ECC than with VCC. As a result, a generally higher diagnostic accuracy for most SLP parameters, except for the NFI, was observed with ECC than with VCC. It is yet unclear whether any future classifiers, specifically developed for ECC images, may outperform the current NFI. Clinically, RNFL images with marked ABPs, acquired with either ECC or VCC, should be used with caution.

References

1. American Academy of Ophthalmology Glaucoma Panel. Preferred practice pattern. Primary open-angle glaucoma. San Francisco: American Academy of Ophthalmology; 2005. Available at: http://www.aao.org/education/library/ppp/poag_new.cfm. Accessed January 18, 2007.
2. Kerrigan-Baumrind LA, Quigley HA, Pease ME, et al. Number of ganglion cells in glaucoma eyes compared with threshold visual field tests in the same persons. Invest Ophthalmol Vis Sci 2000;41:741–8.
3. Quigley HA. Neuronal death in glaucoma. Prog Retin Eye Res 1999;18:39–57.
4. Quigley HA, Addicks EM, Green WR. Optic nerve damage in human glaucoma. III. Quantitative correlation of nerve fiber loss and visual field defect in glaucoma, ischemic neuropathy, papilledema, and toxic neuropathy. Arch Ophthalmol 1982; 100:135–46.
5. Weinreb RN, Dreher AW, Coleman A, et al. Histopathologic validation of Fourier-ellipsometry measurements of retinal nerve fiber layer thickness. Arch Ophthalmol 1990;108: 557–60.
6. Zhou Q, Weinreb RN. Individualized compensation of anterior segment birefringence during scanning laser polarimetry. Invest Ophthalmol Vis Sci 2002;43:2221–8.
7. Greenfield DS, Knighton RW, Huang XR. Effect of corneal polarization axis on assessment of retinal nerve fiber layer thickness by scanning laser polarimetry. Am J Ophthalmol 2000;129:715–22.
8. Reus NJ, van Koolwijk LM, Lemij HG. Effects of inadequate anterior segment compensation on measurements with scanning laser polarimetry. Ophthal Surg Lasers Imag 2006;37:54–7.
9. Reus NJ, Lemij HG. The relationship between standard automated perimetry and GDx VCC measurements. Invest Ophthalmol Vis Sci 2004;45:840–5.
10. Schlottmann PG, De Cilla S, Greenfield DS, et al. Relationship between visual field sensitivity and retinal nerve fiber layer thickness as measured by scanning laser polarimetry. Invest Ophthalmol Vis Sci 2004;45:1823–9.
11. Bowd C, Zangwill LM, Weinreb RN. Association between scanning laser polarimetry measurements using variable corneal polarization compensation and visual field sensitivity in glaucomatous eyes. Arch Ophthalmol 2003;121:961–6.
12. Reus NJ, Lemij HG. Relationships between standard automated perimetry, HRT confocal scanning laser ophthalmoscopy, and GDx VCC scanning laser polarimetry. Invest Ophthalmol Vis Sci 2005;46:4182–8.
13. Medeiros FA, Zangwill LM, Bowd C, et al. Comparison of scanning laser polarimetry using variable corneal compensation and retinal nerve fiber layer photography for detection of glaucoma. Arch Ophthalmol 2004;122:698–704.
14. Medeiros FA, Zangwill LM, Bowd C, Weinreb RN. Comparison of the GDx VCC scanning laser polarimeter, HRT II confocal scanning laser ophthalmoscope, and Stratus OCT optical coherence tomograph for the detection of glaucoma. Arch Ophthalmol 2004;122:827–37.
15. Greaney MJ, Hoffman DC, Garway-Heath DF, et al. Comparison of optic nerve imaging methods to distinguish normal eyes from those with glaucoma. Invest Ophthalmol Vis Sci 2002;43:140–5.
16. Bowd C, Zangwill LM, Medeiros FA, et al. Structure-function relationships using confocal scanning laser ophthalmoscopy, optical coherence tomography, and scanning laser polarimetry. Invest Ophthalmol Vis Sci 2006;47:2889–95.

17. Weinreb RN, Bowd C, Zangwill LM. Glaucoma detection using scanning laser polarimetry with variable corneal polarization compensation. Arch Ophthalmol 2003;121:218–24.
18. Tannenbaum DP, Hoffman D, Lemij HG, et al. Variable corneal compensation improves discrimination between normal and glaucomatous eyes with the scanning laser polarimeter. Ophthalmology 2004;111:259–64.
19. Greenfield DS, Knighton RW, Feuer WJ, et al. Correction for corneal polarization axis improves the discriminating power of scanning laser polarimetry. Am J Ophthalmol 2002;134: 27–33.
20. Bagga H, Greenfield DS, Feuer WJ. Quantitative assessment of atypical birefringence images using scanning laser polarimetry with variable corneal compensation. Am J Ophthalmol 2005;139:437–46.
21. Tóth M, Holló G. Enhanced corneal compensation for scanning laser polarimetry on eyes with atypical polarisation pattern. Br J Ophthalmol 2005;89:1139–42.
22. Sehi M, Guaqueta DC, Greenfield DS. An enhancement module to improve the atypical birefringence pattern using scanning laser polarimetry with variable corneal compensation. Br J Ophthalmol 2006;90:749–53.
23. Knighton R, Zhou Q. Nerve fiber analyzer GDx: new techniques. In: Iester M, Garway-Health DF, Lemij HG, eds. Optic Nerve Head and Retinal Nerve Fiber Analysis. Savona, Italy: Dogma; 2005:117–9.
24. Reus NJ, Zhou Q, Lemij HG. Enhanced imaging algorithm for scanning laser polarimetry with variable corneal compensation. Invest Ophthalmol Vis Sci 2006;47:3870–7.
25. Hoddapp E, Parrish RKII, Anderson DR. Clinical Decisions in Glaucoma. St. Louis: Mosby; 1993:52–61.
26. Weinreb RN, Shakiba S, Zangwill L. Scanning laser polarimetry to measure the nerve fiber layer of normal and glaucomatous eyes. Am J Ophthalmol 1995;119:627–36.
27. Zhou Q, Reed J, Betts RW, et al. Detection of glaucomatous retinal nerve fiber layer damage by scanning laser polarimetry with variable corneal compensation. In: Manns F, Soderberg PG, Ho A, eds. Ophthalmic Technologies XIII. Bellingham, WA: SPIE; 2003:32–41. Proceedings of SPIE Vol. 4951.
28. RNFL Analysis with GDx VCC: A Primer and Clinical Guide. Dublin, CA: Carl Zeiss; 2004:36–6.
29. DeLong ER, DeLong DM, Clarke-Pearson DL. Comparing the areas under two or more correlated receiver operating characteristic curves: a nonparametric approach. Biometrics 1988;44:837–45.
30. Harper R, Reeves B. Compliance with methodological standards when evaluating ophthalmic diagnostic tests. Invest Ophthalmol Vis Sci 1999;40:1650–7.
31. Reus NJ, Lemij HG. Diagnostic accuracy of the GDx VCC for glaucoma. Ophthalmology 2004;111:1860–5.
32. Tjon-Fo-Sang MJ, de Vries J, Lemij HG. Measurement by nerve fiber analyzer of retinal nerve fiber layer thickness in normal subjects and patients with ocular hypertension. Am J Ophthalmol 1996;122:220–7.
33. Choplin NT, Lundy DC. The sensitivity and specificity of scanning laser polarimetry in the detection of glaucoma in a clinical setting. Ophthalmology 2001;108:899–904.